

Femtosecond fabricated photomasks for fabrication of microfluidic devices

Daniel Day and Min Gu

Centre for Micro-Photonics, Faculty of Engineering and Industrial Sciences, Swinburne University of Technology,
Hawthorn, Victoria 3122, Australia
dday@swin.edu.au

Abstract: This paper describes the direct write laser fabrication of a photolithography mask for prototyping of microfluidic devices in polydimethylsiloxane. An amplified femtosecond pulse laser is used to selectively remove the aluminium metal layer from the poly(methyl methacrylate) photomask substrate. The use of a femtosecond pulse laser to selectively etch a metal layer has several advantages over other conventional methods for binary photomask fabrication, namely rapid prototyping of microfluidic devices using soft lithography. Control of the energy density and defocus position of the focusing objective lens results in the etching of features with widths ranging from 2 μm to 35 μm when using an objective lens with a numerical aperture of 0.25.

©2006 Optical Society of America

OCIS codes: (140.3390) Laser materials processing; (320.2250) Femtosecond phenomena; (220.4000) Microstructure fabrication.

References and links

1. M. J. Madou, *Fundamentals of microfabrication: The science of miniaturisation*, 2nd ed., (CRC Press, Boca Raton, 2002).
2. S. Rizvi, *Handbook of photomask manufacturing technology*, (CRC Press, Boca Raton, 2005).
3. S. Saliternan, *Fundamentals of BioMEMS and Medical Microdevices*, (SPIE Press, Bellingham, 2006).
4. D. C. Duffy, J. C. McDonald, O. J. Schueller and G. Whitesides, "Rapid prototyping of microfluidic systems in poly(dimethyl siloxane)," *Anal. Chem.* **70**, 4974-4984 (1998).
5. D. C. Duffy, O. J. Schueller, S. T. Brittain and G. Whitesides, "Rapid prototyping of microfluidic switches in poly(dimethyl siloxane) and their acitiationby electro-osmotic flow," *J. Micromech. Microeng.* **9**, 211-217 (1999).
6. D. Lim, Y. Kamotani, B. Cho, J. Mazumder and S. Takayama, "Fabrication of microfluidic mixers and artificial vasculatures using a high-brightness diode-pumped Nd:YAG laser direct write method," *Lab Chip* **3**, 318-323 (2003).
7. D. Therriault, S. R. White and J. A. Lewis, "Cahotic mixing in three-dimensional microvascular networks fabricated by direct-write assembly," *Nat. Mater.* **2**, 265-271 (2003).
8. D. Day and M. Gu, "Microchannel fabrication in PMMA based on localized heating by nanojoule high repetition rate femtosecond pulses," *Opt. Express* **13**, 5939-5946 (2005).
9. J. C. McDonald, D. C. Duffy, J. R. Anderson, D. Chiu, H. Wu, O. J. Schueller and G. Whitesides, "Fabrication of microfluidic systems in poly(dimethyl siloxane)," *Electroph.* **21**, 27-40 (2000).
10. S. K. Sia and G. Whitesides, "Microfluidic devices fabricated in poly(dimethyl siloxane) for biological studies," *Electroph.* **24**, 3563-3576 (2003).
11. D. B. Wolfe, J. B. Ashcom, J. C. Hwang, C. B. Schaffer, E. Mazur and G. Whitesides, "Customization of poly(dimethyl siloxane) stamps by micromachining using a femtosecond-pulsed laser," *Adv. Mater.* **15**, 62-65 (2003).
12. C. B. Schaffer, A. O. Jamison and E. Mazur, "Morphology of femtosecond laser-induced structural changes in bulk transparent materials," *Appl. Phys. Lett.* **84**, 1441-1443 (2004).
13. M. S. Giridhar, K. Seong, A. Shulzgen, P. Khulbe, N. Peyghambarian and M. Mansuripur, "Femtosecond pulsed laser micromachining of glass substrates with applications to microfluidic devices," *Appl. Opt.* **43**, 4584-4589 (2004).
14. I. H. Chowdhury, X. Xu and A. M. Weiner, "Ultrafast double pulse ablation of fused silica," *Appl. Phys. Lett.* **86**, 151110 (2005).
15. E. N. Glezer, M. Milosavljevic, L. Huang, R. J. Finlay, T. H. Her, J. P. Callan and E. Mazur, "Three-dimensional optical storage inside transparent materials," *Opt. Lett.* **21**, 2023-2025 (1996).
16. D. Day and M. Gu, "Formation of voids in doped polymethylmethacrylate polymer," *Appl. Phys. Lett.* **80**, 2404-2406 (2002).

17. M. Masuda, K. Sugiola, Y. Cheng, N. Aoki, M. Kawachi, K. Shihoyama, K. Toyoda, H. Helvajian and K. Midorikawa, "3-D microstructuring inside photosensitive glass by femtosecond laser excitation," *Appl. Phys. A* **76**, 857-860 (2003).
 18. M. Ventura, M. Straub and M. Gu, "Void channel microstructures in resin solids as an efficient way to infrared photonic crystals," *Appl. Phys. Lett.* **82**, 1649-1651 (2003).
 19. Y. Li, K. Itoh, W. Watanabe, K. Yamada, D. Kuroda, J. Nishii and Y. Jiang, "Three-dimensional hole drilling of silica glass from the rear surface with femtosecond laser pulses," *Opt. Lett.* **26**, 1912-1914 (2001).
 20. K. Venkatakrishnan, B. K. Ngoi, P. Stanley, L. E. Lim, B. Tan and N. R. Sivakumar, "Laser writing techniques for photomask fabrication using a femtosecond laser," *Appl. Phys. A* **74**, 493-496 (2002).
 21. K. Venkatakrishnan, P. Stanley and L. E. Lim, "Femtosecond laser ablation of thin films for the fabrication of binary photomasks," *J. Micromech. Microeng.* **12**, 775-779 (2002).
 22. S. Sowa, W. Watanabe, T. Tamaki, J. Nishii and K. Itoh, "Symmetric waveguides in poly(methyl methacrylate) fabricated by femtosecond laser pulses," *Opt. Express* **14**, 291-297 (2005).
-

1. Introduction

Rapid prototyping of microfluidic device designs is growing in importance, both in terms of time and cost as the microfluidic industry continues to generate new avenues for biological and chemical research. The fabrication of photomasks is still a fundamental step in the development of microfluidic devices, regardless of the method used for device replication. Typically high resolution photomasks are fabricated using a photolithographic or e-beam lithographic process [1-3] in order to achieve features with dimensions less than a micrometer. However, both lithographic fabrication methods rely on the use of a photoresist for transferring an image to a photomask. When a photoresist is used to generate a photomask multiple steps are required just to produce the photomask, which then in turn can be used to replicate the designed structure. The disadvantage of using conventional photolithography or e-beam lithography is the time and expense required to produce a new photomask. This becomes apparent during the development cycle of a device, where the frequent redesign of structures or geometries requires repeated fabrication of the photomask. Recently we have seen the emergence of high resolution printing as an alternative method for generating a photomask for microfluidic device manufacturing [4, 5]. Generally microfluidic devices require feature resolutions on the order of a micrometer with total combined channel lengths of at least centimeters.

A microfluidic device can be fabricated using any number of methods other than lithography. Micromachining with excimer and Nd:YAG lasers is the most common method for micromachining; however the nanosecond pulse width generated by those lasers results in the formation of a large heat affect zone (HAZ). Depending on the material being machined, fabrication defects such as cracks can appear in the HAZ and ejected debris can be found around the interaction region. Moreover, the selective etching of a metal layer or layers from the surface of a transparent substrate is not possible with excimer or Nd:YAG lasers. Direct write fabrication of microchannels has been demonstrated using a Nd:YAG [6], assembly of organic inks [7] and a femtosecond laser [8]. While direct write fabrication can be used to fabricate two- and three-dimensional microchannels directly in a range of different substrates, the drawback occurs when replication of the microfluidic system is required. Whereas the cost of a complex photomask is seen as prohibitive, the cost of a serial direct write fabrication method would preclude it from being used to replicate a commercial microfluidic device.

The advantage of developing a photomask becomes apparent when consideration is given to the method to be used for replicating the microchannels. Soft lithography with poly(dimethylsiloxane) (PDMS) is a desirable process as PDMS has been demonstrated to be a suitable material for biological [9-11] microfluidic applications and for the ease with which microfluidic devices can be replicated in PDMS without destroying the master mold. Another advantage of using PDMS is the method required to replicate the devices can be accomplished without expensive equipment compared with hot embossing.

Femtosecond pulse lasers are finding more applications in micromachining due to their ability to fabricate in a wide range of materials with little or no heating or damage outside the focal spot [11-13]. Applications of femtosecond micromachining include surface ablation [14], optical data storage [15, 16], optical waveguides, micro-optical components [17],

photonic band gap structures [18] and microfluidic channels [19]. The short pulse width of femtosecond lasers provides a means of micromachining metals and dielectrics without defects and debris that are typically associated with a build up of heat in the focal region. The energy density that is created from focusing mJ femtosecond pulses ($> 10^{15} \text{ W cm}^{-2}$) typically results in the ionisation of the material in the focal region. The creation of a plasma in the focal region transfers the energy and heat away from the surrounding material, resulting in a HAZ that is limited to the extent of the focal region. As fabrication using femtosecond pulses is predominately a nonlinear process the material ablation occurring within the focal region can be controlled by adjusting the pulse energy within the focal spot, known as 'thresholding'. This can result in the production of features with dimensions below the diffraction limit of the focusing optics used [12]. When layering a number of dissimilar materials with different optical breakdown thresholds individual materials can be machined without affecting the surrounding materials. Femtosecond pulse lasers have been used to directly write a pattern into a gold and chromium coated quartz substrate in order to produce photomasks [20, 21].

In this paper we report on the use of femtosecond pulse lasers to selectively etch the aluminium metal layer on a poly(methyl methacrylate) (PMMA) substrate in order to fabricate a binary photomask for the rapid prototyping of microfluidic devices using soft lithography. This method of producing photomasks can simplify the number of steps required to fabricate a microfluidic device and therefore reduce the time and cost associated with developing new devices.

2. Experimental setup

The photomask substrate consists of a PMMA substrate cut to the size of a glass slide (75 mm x 25 mm) with a thickness of 2 mm. A metal layer of aluminium (Al) was coated onto one surface of the PMMA using evaporation vacuum deposition (EMITECH). The thickness of the Al layer was controlled in order to limit the transmission of the ultra-violet light from the Mercury lamp used to polymerise the photoresist during fabrication of the master mold. A layer thickness of 250 nm was found to remove sufficient ultra-violet light from a focused 100 W Mercury lamp.

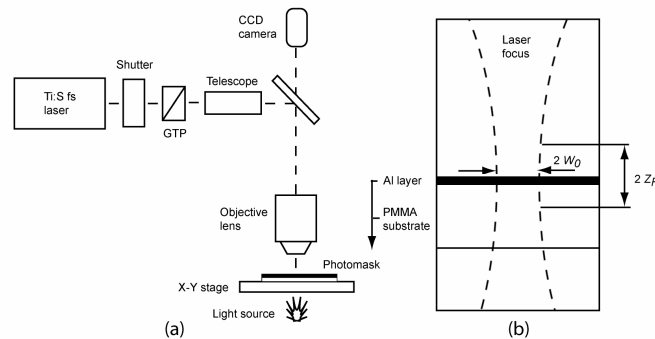


Fig. 1. (a). Schematic illustration of the optical setup. (b). An illustration showing the focused femtosecond laser beam and its focus position relative to the metal layer. The beam waist in the focus is represented by w_0 and the Rayleigh range is indicated by z_R .

Fabrication of the photomask is achieved with an amplified Ti:Sapphire femtosecond (fs) pulse laser (Spitfire, Spectra Physics) that produces 100 fs pulses at a repetition rate of 1 kHz at a wavelength of 800 nm. The beam first passes through a mechanical shutter for controlling the exposure and a Glan Thompson prism (GTP) for controlling the intensity, before being directed through a telescope to expand the beam to match the back aperture of the objective lens. A 0.25 numerical aperture (NA) objective lens is used to focus the laser onto the sample. The objective lens is mounted on a vertical translation stage, while the sample is mounted on an x-y translation stage. A white light source and CCD camera are

mounted to monitor the fabrication in situ. Mounting the white light source in transmission mode allows real time inspection of the quality of the metal layer removal, by observing the quality of the light being transmitted through the newly etched regions. A schematic of the experimental setup used to fabricate the photomask is illustrated in Fig. 1(a).

The removal of the Al layer occurs in the focal spot of the objective lens where the energy density is sufficient to directly ionise the Al layer. From Fig. 1(b) it can be seen that the Rayleigh range (z_R) of a 0.25 NA objective lens extends beyond the metal layer into the PMMA substrate. By controlling the energy in the focal spot and utilising the different optical and mechanical properties of the two materials a threshold can be determined whereby the Al layer is removed without destroying the underlying PMMA layer. The Rayleigh range and focus diameter ($2 w_0$) for the 0.25 NA objective lens are 11 μm and 2 μm , respectively.

A photomask is fabricated under atmospheric conditions, which results in the redeposition of some of the removed material. It has been shown that micromachining of different materials under a vacuum results in improved ionisation of the target material and little or no redeposition or debris [21]. However, fabricating under vacuum conditions increases the time and complexity of the fabrication of the photomask and is only required when fabricating nanometer size structures.

3. Results and discussion

3.1 Effect of energy thresholding

The ability to select different materials for removal using femtosecond pulse laser fabrication is a unique characteristic of the physical processes associated with a femtosecond temporal pulse. The direct ionisation of a specific material in the focal region within a single or multiple pulses results in the removal of that material with limited temperature build up or transfer to the surrounding material.

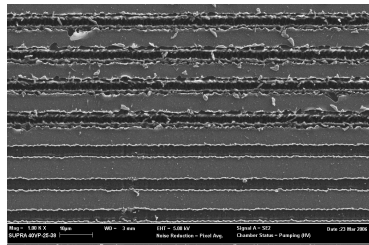


Fig. 2. SEM image of a series of lines fabricated at different energies. The top four lines are fabricated with a fluence (5 J/cm^2) above the threshold for ionising the PMMA substrate while the bottom three lines are fabricated with a fluence (0.7 J/cm^2) where only the Al layer is ionised.

A scanning electron microscope (SEM) image (Fig. 2) of a series of lines fabricated in the sample at different energies show that by controlling the energy per pulse, the metal layer can be removed without damaging the underlying PMMA substrate. The energy density required to ablate the PMMA when the objective was focused on the surface of the photomask was 5 J/cm^2 . When the energy density is reduced to 0.7 J/cm^2 the Al layer is removed while leaving the PMMA substrate unaffected. At energies below the ionization threshold modification of the optical properties of PMMA can still occur [23]. The width of the line generated by the removal of the Al layer is $3.8 \mu\text{m}$, while the width of the channel ablated in the PMMA is $1.9 \mu\text{m}$. The use of thresholding when fabricating photomasks using femtosecond pulse lasers is important as any damage to the PMMA substrate reduces the quality of the UV transmission which in turn affects the fabrication of the master. A feature that can be seen in Fig. 2 is the ripple along the edges of the fabricated regions. The ripple is due to the overlap between successive pulses as the sample is translated. In order to remove the ripples more overlap between the successive pulses would be required which can be achieved by slowing the

translation speed of the sample. Another characteristic that can be observed is the lack of debris surrounding the fabrication of the metal layer. For the fabrication conditions used to remove the Al layer, the energy density was sufficient to almost completely ionise the metal layer limiting the debris or redeposition of Al.

3.2 Effect of defocusing

By controlling the focal position of the focused femtosecond pulses with respect to the surface of the metal layer, the amount of metal that is ionised per pulse can be changed. As it is the energy density that is most significant in terms of whether the material is ionised or not, any change in the focal position will also change the energy density incident on the metal layer. Using this method of defocusing two effects can be achieved. The first is that a larger area of material can be removed per pulse and second, defocusing changes the tolerances associated with removing the metal while not affecting the substrate. It can be seen from Fig. 3 that by moving the focal position away from the sample surface the area that is irradiated by the beam is increased. The defocus distance (Δz) is given as the distance between the focused beam waist and the metal layer. Figure 3(a) illustrates focused conditions ($\Delta z = 0$) while Figs. 3(b) and 3(c) illustrate 45 μm and 75 μm defocus conditions. Figure 3(d) illustrates the theoretical and experimental width of an etched line based on the defocus position. Also, within the focal spot the energy density is a Gaussian distribution, with the highest energy located at the centre of the focal spot. Whereas the energy density outside of the Rayleigh range is relatively uniform across the beam in comparison to that in the focal spot. By defocusing the fabrication beam more control over the energy density irradiating the sample can be achieved, which reduces the likelihood of ionising the substrate.

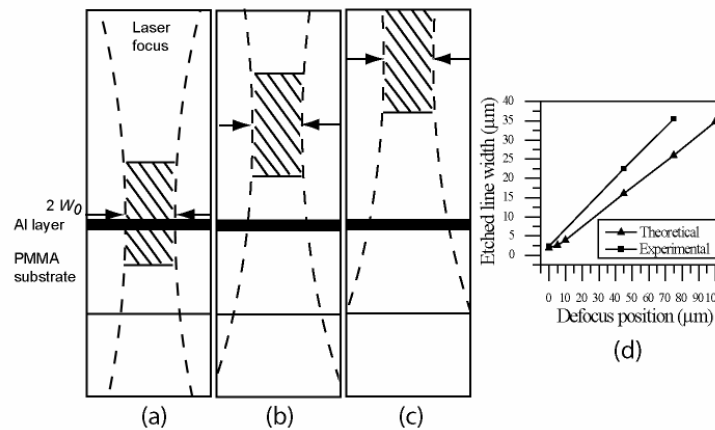


Fig. 3. Schematic diagram representing the defocus position of the objective lens and the limit of the Rayleigh range with respect to the Al layer. (a) the objective is focused on the metal layer, (b) the objective lens is defocused by 45 μm and (c) the objective lens is defocused by 75 μm . The Rayleigh range is indicated by the hashed region. (d) illustrates the theoretical and experimental values for the width of the etched line as a function of defocus position.

The effect of defocusing on the removal of an Al layer can be seen in Fig. 4. In Fig. 4 a series of lines were fabricated where the metal layer has been removed under (a) focused, (b) 45 μm defocus and (c) 75 μm defocus conditions. The widths of the lines fabricated as a result of the focus, 45 μm defocus and 75 μm defocus conditions are 2.4 μm , 22.5 μm and 35.4 μm , respectively. Theoretical predictions of the beam width corresponding to the three defocus positions are 1.9 μm ($\Delta z = 0$), 16 μm ($\Delta z = 45 \mu\text{m}$) and 26 μm ($\Delta z = 75 \mu\text{m}$). The energy density used to remove the Al layer was 0.7 J/cm^2 and the sample was translated at a speed of 800 $\mu\text{m}/\text{s}$. From Figs 4(a), 4(b) and 4(c) it can be seen that the energy density is

significant enough to ionise the metal layer without affecting the substrate, however in Fig. 4(c) the energy density is reduced to 0.3 J/cm^2 such that not all the metal layer can be ionised. It is clear that the edges of the remaining metal were melted rather than ionised. This is also confirmed by the significant quantity of debris that can be seen in the image.

Fabrication of a photomask by selectively removing the metal layer from a PMMA substrate can be used to increase the speed of development of microfluidic devices. An example of a device that is fabricated using this method of fabricating a photomask is shown in Figs. 4(d) and 4(e). The completed and sealed y-junction microfluidic device can be seen in Fig. 4(d) with a fluorescence image of the laminar flow shown in Fig. 4(e). The final channel dimensions are width $100 \mu\text{m}$, depth $100 \mu\text{m}$ and length 13.5 mm . By controlling the defocus during the fabrication process the time taken to produce the photomask can be reduced. For the case of the y-junction photomask the fabrication time was less than 5 minutes.

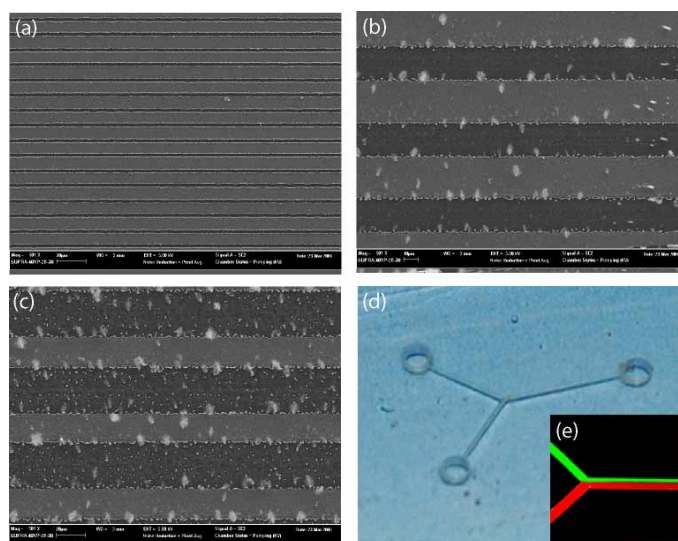


Fig. 4. Fabrication of a photomask using defocusing. SEM images of a series of lines fabricated at different objective lens defocus positions, (a) $\Delta z = 0 \mu\text{m}$, (b) $\Delta z = 45 \mu\text{m}$ and (c) $\Delta z = 75 \mu\text{m}$. (d) a sealed y-junction microfluidic device. The length of the microfluidic channels from the inlets to the outlet is 13.5 mm and the channel width and depth are both $100 \mu\text{m}$. (e) a two-colour fluorescence image showing the laminar flow produced in the y-junction microfluidic device.

4. Conclusion

The production of photomasks for microfluidic devices is an expensive exercise both in time and cost, which does not allow any flexibility for iterative development cycles. The ability to selectively remove a metal layer from an optically transparent substrate using femtosecond pulsed lasers provides a means of directly transferring the pattern to the photomask. By controlling the energy density and defocus position of the focused femtosecond pulses the photomask can be generated in minutes which is suitable for producing a master for replication using PDMS. The ability to change the focus position and therefore change the amount of the metal layer removed ensures that both high and low resolution features can be achieved in the photomask. This method of producing a photomask also provides a method for modifying a photomask which could lead to faster microfluidic device development times.

Acknowledgments

The authors would like to acknowledge the support from the Australian Research Council.